ISSN 0003-6838, Applied Biochemistry and Microbiology, 2024, Vol. 60, No. 4, pp. 676–685. © Pleiades Publishing, Inc., 2024.

Platinum Nanoparticles in Aqueous Solutions of a Chitosan–Vinylpyrrolidone Copolymer: Synthesis and Biological Activity

D. N. Zuev[a], *, E. I. Cherkasova[a], K. V. Apryatina[a], S. D. Zaitsev[a], and L. A. Smirnova[a]

[a] *National Research Lobachevskii Nizhny Novgorod State University, Nizhny Novgorod, 603022 Russia*

**e-mail: z_u_e_v2020@mail.ru*

Received January 30, 2024; revised February 21, 2024; accepted February 28, 2024

Abstract—Grafted copolymers of chitosan–vinylpyrrolidone, water-soluble at a pH of 6.8–7.5, were obtained. A technique has been developed for obtaining an aggregatively stable system of platinum nanoparticles in copolymer solutions with an average size of ~4 nm. The thermophysical and structural characteristics of the powdered composition of a platinum nanoparticle-copolymer are investigated. An in vitro comparison of the antitumor activity of solutions of the developed composition and cisplatin at the same platinum concentration was performed. It was found that with respect to the culture of HeLa Kyoto and A431 cancer cells, the composition is five and two times less effective than cisplatin, respectively. Along with this, the biocompatibility of the composition is 17 times higher than that of cisplatin, which allows its use at elevated concentrations and the development of an antitumor agent with platinum nanoparticles commensurate in effectiveness with cisplatin.

Keywords: chitosan–graft–polyvinylpyrrolidone, platinum nanoparticles, water-soluble composition, antitumor properties, biocompatibility

DOI: 10.1134/S0003683824604451

In the past two decades, nanotechnologies have been rapidly developing in all directions as a result of significant changes in the properties of materials when nanoparticles (NPs) are introduced into them. In biomedicine, NPs of metals, in particular, noble metals (silver, gold, and platinum) are studied with respect to the treatment and prevention of various diseases, including cancer, human immunodeficiency virus, tuberculosis, and Parkinson's disease, and are promising for drug delivery [1, 2]. In view of the above, much attention has been focused on the toxicological and therapeutic effects of NPs, depending on the concentration, size, and shape of the latter [3]. The shape and size of metal NPs can be controlled by using stabilizers of different natures [4, 5]. Promising stabilizers are biopolymers that have intrinsic biological activities and, in complex with NPs, can manifest synergistic properties and increase the therapeutic effects of the latter [6].

The most in-demand area of platinum NP studies is the synthesis of antitumor drugs [7–12]. There are a lot of drugs for treating oncological pathologies, and still more drugs are at the stage of development. Although there are some very promising agents among this great number of drugs being produced, they often cannot pass clinical trials because they are toxic or hard-to-dissolve under physiological conditions.

Platinum-containing chemotherapeutic drugs are effective, but their applications are associated with serious dose-dependent side effects and enhanced drug resistance, which can increase even more after exposure to chemotherapeutic agents [13–17].

Platinum-based drugs still remain the basic agents used in chemotherapy for some types of cancer, mainly as Pt^{II} coordination complexes such as cisplatin, carboplatin, oxaliplatin, nedaplatin, lobaplatin, and heptaplatin. Platinum-based drugs are the most efficient chemotherapeutic agents for treating non-small-cell lung cancer, being recommended as line 1 agents in its therapy. Study [18] has shown that the therapeutic schemes not including platinum agents are accompanied by a decrease in the treatment efficiency and in the median survival to one year. Currently, cisplatin is the most widespread and efficient agent. It is a crystalline powder, which is dissolved in water and used as injections. Structurally, cisplatin consists of the central platinum atom, which is bound to two chloride and two ammonia groups. It is used to treat different types of cancer, such as lung cancer, ovarian cancer, bladder cancer, etc.

Cisplatin is able to interact with cellular DNA. It binds preferentially to nucleotides, first of all adenine and guanine, causing different changes in the DNA structure such as deformations of the DNA double helix, crossing, interstrand cross-links, and strand

breaks [19]. The interaction between cisplatin and DNA leads to the impairment of its structure and the blockade of cell division. Cisplatin causes cell cycle arrest in the G1-, S-, or 62-phase. Most likely, the arrest in the G2-phase is necessary for triggering cisplatin-induced cell death.

However, cisplatin can cause various side effects: nausea, vomiting, diarrhea, hair loss, etc. In addition, there may be loss of function in the kidneys and in the nervous system [20].

Platinum nanoparticles (NPs) are widely used for biomedical applications, inter alia, as implant components, in photothermal therapy, and for drug delivery. In order to decrease the toxicity and to increase the biocompatibility of antitumor drugs, it would be relevant to develop new modified complexes on the basis of platinum NPs. The increased reactivity of NPs in biological environments can lead to the death of tumor cells. Platinum can be cytotoxic when oxidized to platinum (II); in this form, it occurs in the common chemotherapeutic drugs [21]. For example, many NPs interact with cells with the formation of reactive oxygen species that can lead to the untimely death of tumor cells. This property can be used for suppression of the latter [22].

Compared to the conventional clinical platinum agents, platinum NP-based drugs have demonstrated high stability and solubility in vitro, as well as low systemic toxicity and biocompatibility in vivo. The studies of the efficiency of platinum NPs show that they per se are nontoxic for healthy human cells at therapeutic concentrations and can be used at higher concentrations for tumor therapy [23]. Platinum NPs have intrinsic antimicrobial, antioxidant, and anticancer properties. Thus, platinum NPs are highly promising to be studied and used in nanomedicine and in biomedical engineering [24].

One of the problems associated with successful application of antitumor drugs is that active agents have low molecular weights and therefore do not penetrate the target organ and do not reach tumor tissues or cannot penetrate into them. This problem can be solved by including medicinal agents into a "capsule." NPs stabilized by a polymeric matrix/carrier will be adsorbed on tumor tissues and get inside. One such promising polymer for creating drug delivery systems is chitosan, the deacetylated derivative of the natural polysaccharide chitin. Chitosan is a universal sorbent that can bind a huge range of organic and inorganic substances [25]. It is also biodegradable, biocompatible, and nontoxic. Chitosan has reactive groups (a hydroxyl group and an amino group) in each link, allowing the chemical attachment of several molecules required for particle functionalization. Such a structure of chitosan makes it possible to obtain derivatives with different charges and hydrophobicity [26]. Article [27] describes studies of chitosan-based NPs used for the delivery of chemotherapeutic agents. Such delivery systems increased the solubility and bioavailability of the agents under study. For example, cisplatin was encapsulated in a chitosan-modified magnetite NP. Such NPs had a cytotoxic effect on the MDA-MB-231 human breast cancer cell line, and it was higher than in cisplatin not encapsulated in NPs.

The disadvantage of the chitosan-based matrix as a carrier is its solubility at pH below 5, while the blood and the lymph fluid have a pH value of 7. One of the solutions is chitosan modification by water-soluble and biocompatible polymers such as polyvinylpyrrolidone (PVP). PVP is also often used as a NP carrier; it prevents their uncontrolled growth and aggregation. Different NPs stabilized by PVP can be promising for biomedical applications. For example, in work [28], gold NPs were synthesized with PVP used as a stabilizer. Such NPs were toxic for HeLa cells. The disadvantage of this polymer is the possibility of its hydrolysis. Works [29, 30] have shown that vinylpyrrolidone (VP) in acidic media can be hydrolyzed with the formation of α-oxyethylpyrrolidone. This problem can be solved by optimizing the conditions of copolymer synthesis to the minimum concentration of the hydrolysis product or the use of an aprotic solvent that completely eliminates hydrolysis.

The aim of this work was to obtain a water-soluble chitosan–graft–PVP composition with platinum NPs and to study the properties of the system.

MATERIALS AND METHODS

Chitosan used in this study was obtained from crab shell chitin (Bioprogress, Russia) and had a molecular weight (MW) of 2.20×10^5 and deacetylation degree of 0.82. The mass fraction of minerals in chitosan was no more than 0.1%; the moisture content was 6%; and insoluble compounds made up 0.1%.

Chitosan solutions were prepared using "chemically pure" glacial acetic acid, GOST 61-75. Chitosan was modified by graft polymerization with N-vinyl-2-pyrrolidone (Acros Organics, Belgium) prepurified by vacuum distillation.

Dimethylsulfoxide (DMSO) was "chemically pure," Company Standard STP TU KOMP 2-451-11 (Component-Reaktiv, Russia). Salicylic acid was of the "chemically pure" grade (Vekoslab, Russia).

Platinum NPs were obtained from the precursor: chloroplatinic acid 6-hydrate ($H_2PtCl_6 \cdot 6H_2O$) of the "pure" grade (Aurat, Russia); the mass fraction of platinum was no less than 37.5%. Sodium borohydride, $NaBH_4$, was used as a reducer of platinum ions.

The graft copolymerization of VP onto chitosan was performed in a three-neck round-bottom flask equipped with a reflux condenser, which was placed into a thermostat with regulated temperature, under continuous stirring. The chitosan concentration in the acetic acid solution in all experiments was 3 wt %; the acetic acid concentration was 1.2 wt %; reaction tem-

perature was 70°C. Chitosan concentration in dimethylsulfoxide in all experiments was 1.5 wt %; salicylic acid was 1.5%; and the reaction temperature was 70°C. NPs were introduced into the system after setting the reactor temperature at 70°C and argon barbotage for 15 min. The [monomer]/[chitosan] mass ratio was 4. Ammonium persulfate and ceric ammonium nitrate were used as initiatory systems in both aqueous and dimethylsulfoxide solution. The system was kept for 15 min to establish the required temperature of the solution, followed by the addition of a weighed portion of the initiator. The concentration of initiators was 10^{-3} mmol/L. The synthesis was performed for 3 h until the process of VP polymerization was completed.

The depth of VP conversion was determined by the results of the analysis of the residual monomer by gas chromatography.

The concentration of the residual monomer was determined with a GCMS-QP2010 gas chromatograph, Shimadzu (Japan), with a thermal conductivity detector and a computerized recording system. The column was Equity-1 (30 m, 0.25 mm, 0.25 μm); and the carrier gas was helium. The carrier gas flow rate in the column was 1 mL/min; the column temperature for determination of the VP content was 230°C. Samples were taken from the reaction system every 30 min; the polymers contained in the samples were precipitated with tetrahydrofuran. The sample-to-precipitator ratio was 100 mg per mL. Then the supernatant was filtered through a PTFE membrane filter (Merck, Millipore), 0.45 μm, and the VP content was determined by gas chromatography.

The molecular weight distribution of polymer samples was performed by the method of gel penetrating chromatography (GPC) using a Prominence UFLC Fast LC-20AD high-performance liquid chromatograph (Shimadzu, Japan). The conditions of analysis were the following: eluent, 0.5 n acetic acid solution; flow rate, 0.8 mL/min; T = 30°C; detector, ELSD (low-temperature evaporative light-scattering detector). The column was TSK-GEL G3000SWXL, 7.8 mm ID × 30.0 cm L, 5 μm. Calibration was performed using narrowly dispersed dextran samples within a MW range from 1000 to 410000 Da.

Platinum NPs were obtained in chitosan hydroacetate solutions (3 wt%) and in aqueous chitosan–graft–PVP solutions by reducing Pt^{4+} ions from dopant H_2PtCl_6 using sodium borohydride $NaBH_4$ (0.5 M) as a reducer. H_2PtCl_6 was added to 0.5 wt % of aqueous solution of the copolymer under continuous stirring, so that the NP concentration was 2% Pt of the copolymer, and thermostated at 70°C for 30 min. The absorption spectrum was recorded relative to 0.5% aqueous solution of the copolymer diluted with 19 parts of water in a Shimadzu UV-1650PC spectrometer. Pt^{4+} reduction was accompanied by the appearance and enhancement of the plasmon absorption band typical of platinum NPs in the wavelength region of 210–230 nm [31].

The X-ray phase analysis (XPA) of the samples was performed with a Bruker D8 Discover X-ray diffractometer (Germany) using CuKα radiation. Diffractograms were recorded for the angular range of 10°–60° at a diffraction angle of 2θ in symmetrical geometry with a slot of 0.6 mm for the primary beam and with a linear LynxEye position sensitive detector (Bruker, Germany).

The thermophysical properties of the samples were studied by the method of differential scanning calorimetry (DSC) using a DSC 500 system (Laboratory of Analytic Instruments and Systems, Samara State Technological University, Russia). The samples were measured in a nitrogen atmosphere at a heating rate of 10°C/min. Before the analysis, the samples were heated to 105°C in the nitrogen atmosphere to remove traces of water.

The size and crystalline structure of platinum NPs were studied by transmission electron microscopy (TEM) in ultrathin polysaccharide films with a LIBRA 200 MC field-emission microscope (Carl-Zeiss SMT, Germany). For sample preparation, a drop of the solution was applied onto a thin (30 nm) Si_3N_4 membrane followed by centrifugation at ~2000 rpm. After that, polymeric films were treated in mild oxygen plasma using a De-Contamination RF Evactron 25/45 RF plasma cleaning system (United States). This treatment was used to remove the organic matrix from the samples. TEM images were obtained and processed with the Digital Micrograph software (Gatan, Inc., Pleasanton, California, United States).

Additionally, the size and morphology of platinum NPs on the surface of polymeric composite films were characterized by scanning electron microscopy (SEM) with a JEOL JSM-IT300LV system (United States) equipped with elemental analyzers for energy and wave dispersion.

Cytotoxicity against tumor cells in the drugs containing platinum NPs was determined by the methyl thiazole tetrazolium (MTT) test. The MTT test is based on the ability of NADPH-dependent oxidoreductase dehydrogenases of viable cells to convert water-soluble 3-(4,5-dimethylthiazol-2-yl)-2,5-diphenyltetrazolium bromide into formazan crystals. A431 and HeLa Kyoto cells were inoculated into 96-well microplates, 3×10^3 cells/well. After two-day cultivation, the initial medium was replaced by a fresh medium containing preparations at different concentrations. Incubation with the preparation was performed for 24 h in a CO_2 incubator (37.0°C, 5% CO_2); then the cells were washed in a sodium phosphate buffer solution, and 200 μL of the medium containing 0.5 mg/mL of MTT was added into each well. The cells were placed again into a CO_2 incubator for 4 h, and then the medium with MTT was sampled. The resultant formazan was lyzed with the DMSO solution

added by 100 μL per well. The optical density of the resultant formazan solution in DMSO was measured with a Synergy MX microplate spectrophotometer (BioTek, United States) at a wavelength of 570 nm.

The growth and adhesion of hTERT BJ-5ta human fibroblast cells (provided by the Shemyakin and Ovchinnikov Institute of Bioorganic Chemistry, Russian Academy of Sciences, Russia) on the surface of chitosan/platinum NP composite films were studied. Films were obtained in advance by pouring the initial solutions onto a lavsan substrate under the conditions of uniform evaporation of the solvent to a constant weight at 25°C. The films of the composites sterilized by autoclaving at 110°C were placed into microplate wells for cell cultivation, with the addition of 500 μL of the DMEM medium. Cells were inoculated on the film surface at a density of 1.6×10^5 cells/cm^2 and cultivated for 24 h. Fluorescence microscopy was used for cell visualization and cell viability assay. The dye for staining fibroblasts was 2×10^{-4}% acridine orange solution in a phosphate buffer. This dye, through intercalation or electrostatic attraction, selectively interacts with DNA and RNA, which are present in the cell nucleus and mitochondria, respectively. Hence, it is possible to assess the general state of cells: activity, proliferation, and apoptosis. The films were analyzed with an Olympus IX71 inverted microscope (Japan) using a "green" filter (emission, 510–555 nm; excitation, 460–495 nm), which made it possible to visualize the green color in the nucleus of living cells.

RESULTS AND DISCUSSION

With the purpose of obtaining biocompatible and water-soluble chitosan, the latter was modified by VP using graft polymerization. Graft polymerization of VP onto chitosan was performed in aqueous acidic solutions and DMSO (Fig. 1). It is known that VP is hydrolyzed in aqueous acidic solution with the formation of pyrrolidone by the scheme presented in Fig. 2.

Indeed, the results of chromatographic analysis of the products of synthesis demonstrated that up to 6% VP is hydrolyzed during polymerization with the formation of pyrrolidone (Fig. 3): the peak with the release time of 9.89 min corresponded to the monomer, while the peak of 9.28 min corresponded to the product of hydrolysis, i.e., pyrrolidone.

Graft polymerization in water at 70°C with the involvement of initiators such as ammonium persulfate and ceric ammonium nitrate was achieved already within 1.5 h at a conversion of 99%; however, the

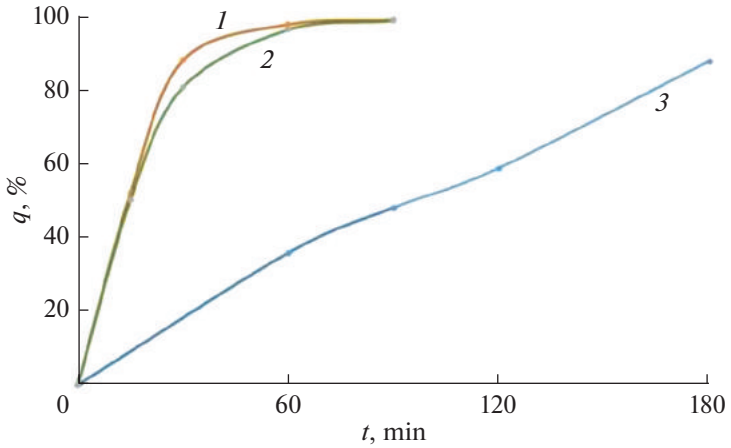

Fig. 1. VP conversion during graft polymerization: (*1*) in an aqueous solution at 70°C with ceric ammonium nitrate as the initiator; (*2*) in an aqueous solution at 70°C with ammonium persulfate as the initiator; and (*3*) in a DMSO solution at 70°C with ceric ammonium nitrate as the initiator.

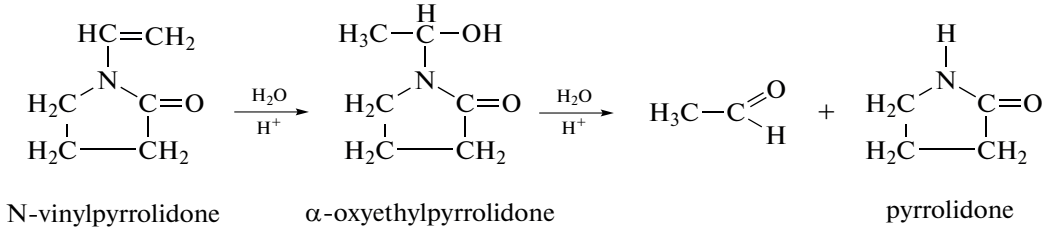

Fig. 2. The reactions of acidic hydrolysis of VP.

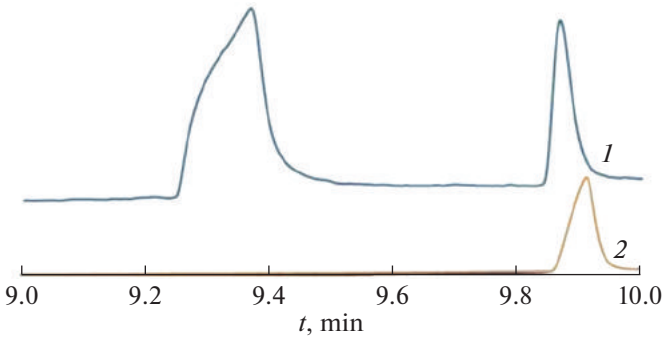

Fig. 3. Chromatograms–samples, (*1*) after the synthesis of polymer separation and (*2*) VP.

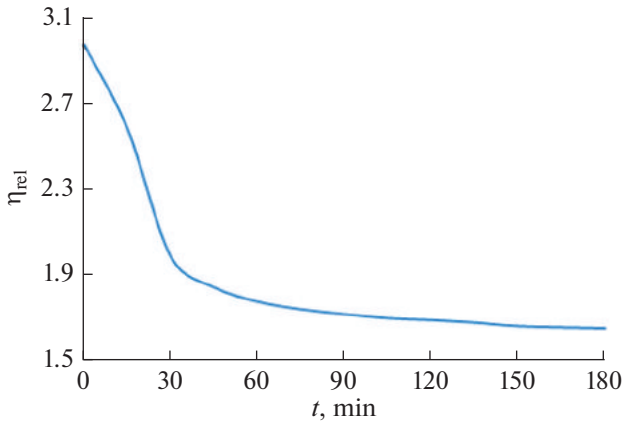

Fig. 4. The decrease in the relative viscosity of the chitosan solution under exposure to ammonium persulfate at 70°C at the initiator concentration of 5×10^{-3} mol/L.

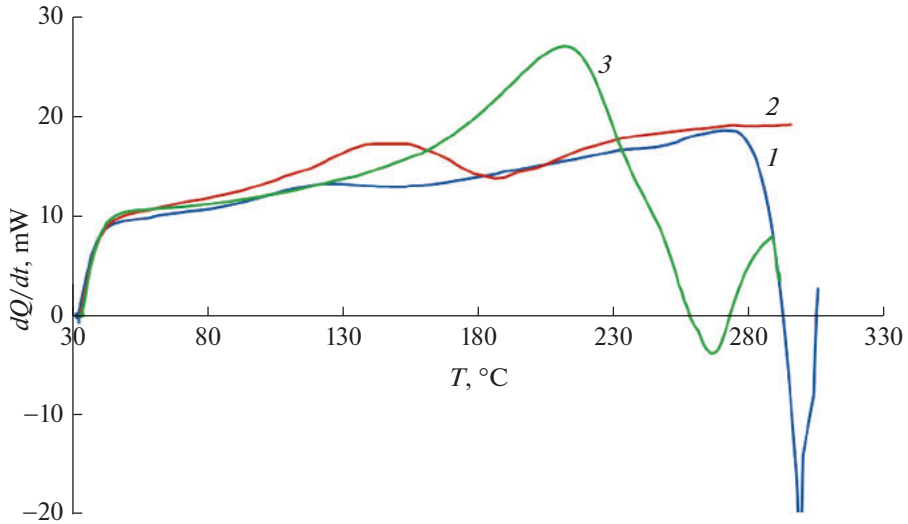

Fig. 5. The curves obtained by DSC: *1*, chitosan; *2*, PVP; *3*, chitosan–graft–PVP.

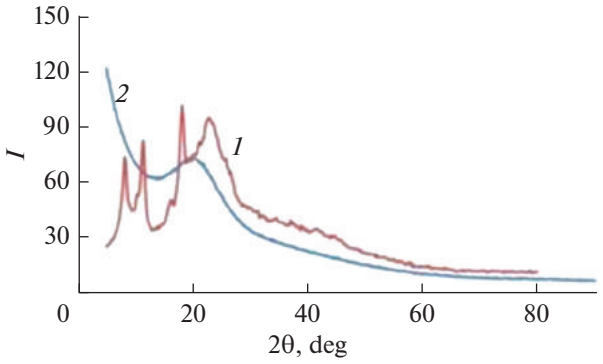

Fig. 6. The XPA spectra of (*1*) chitosan and (*2*) chitosan–graft–PVP.

product of VP hydrolysis also appeared in the reaction mixture.

The molecular weight characteristics of chitosan–graft–PVP copolymer and grafted VP chains were studied by the method of GPC. The MW of grafted VP chains in the copolymer was determined by enzymatic degradation of chitosan chains by chitosanase (Weifang Yuexiang Chemical Co., China). Chitosanase was added to the copolymer solution at a chitosan–chitosanase ratio of 2 : 1 (by weight). Chitosanase is an enzyme specifically cleaving β-1.4-glycoside bonds between D-glucosamine residues, as well as between D-glucosamine and N-acetylglucosamine residues in chitosan molecules, followed by the formation of oligomers. The reaction mixture was kept at 50°C and left to stand for 6 h for the complete cleavage of the polysaccharide. For enzyme inhibition, the solution was heated at 75°C for 3 h. The GPC technique was used to determine the MW of PVP blocks remaining in the solution. Two fractions were isolated; the MWs of grafted VP chains were 1.16×10^4 and 2.55×10^4.

It is known that initiators such as ammonium persulfate and ceric ammonium nitrate cause destruction of the polysaccharide chain of chitosan, and a block copolymer can be produced during polymerization (Fig. 4) [32, 33].

The thermophysical properties of the copolymer and the initial homopolymers were studied to confirm the copolymer structure (Fig. 5). As is known, two glass transition temperatures were observed for the block copolymers but only one for the grafted copolymer [34].

It should be noted that the copolymer sample had a glass transition temperature of 180°C. The lower glass transition temperature of the copolymer (T_g = 180°C) relative to the initial chitosan (200°C) could be due to the reduced crystallinity of the copolymer.

The X-ray phase analysis (XPA) of the copolymer structure was performed to demonstrate the reduced degree of crystallinity. Figure 6 shows that the copolymer has no crystalline peaks typical of chitosan and there is an amorphous halo. The degree of crystallinity of the initial chitosan is calculated as the ratio of the area of crystalline peaks to the total area of the scattering curve: 50.5%. This fact suggests that graft polymerization has been successful and the copolymer is more amorphous than the initial chitosan.

Platinum NPs were obtained in the water-soluble copolymer. The dimensional characteristics of NPs in the copolymer solution were determined in comparison with NPs obtained in the initial chitosan solution. According to the UV spectroscopy data (Fig. 7), chitosan solutions exposed to radiation demonstrated a regularly stable increase in the band maximum at λ = 215 nm, corresponding to the surface plasmon resonance of platinum NPs that reaches a constant value in 30 min. In an aqueous solution of the copolymer, the maximum of the surface plasmon resonance band is at λ = 219 nm. As is known, the more the maximum of the surface plasmon resonance shifts to the long-wavelength band, the larger the NP size is. Thus, the platinum NPs formed in the copolymer are larger compared to chitosan.

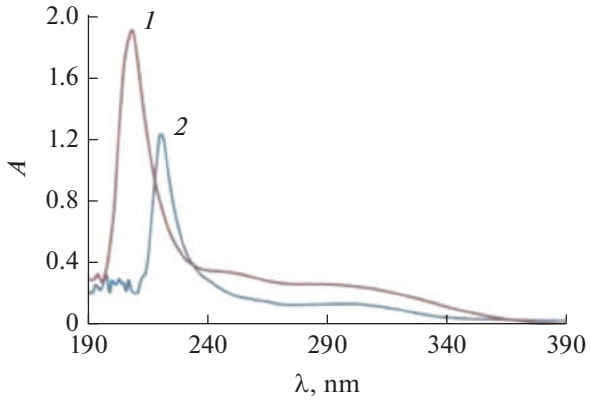

Fig. 7. The UV absorption spectra of platinum NPs in the aqueous acidic solutions (*1*) of chitosan and (*2*) in the aqueous solutions of the copolymer.

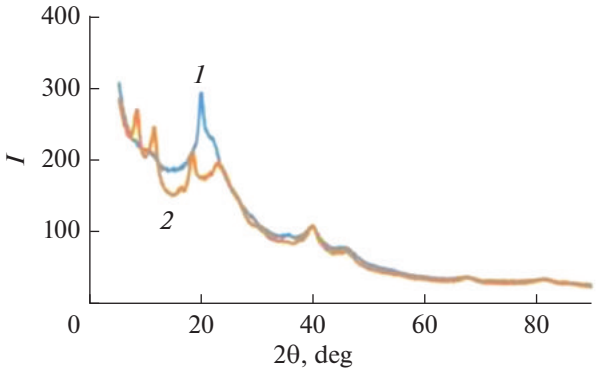

Fig. 8. The XPA spectrum of platinum NPs (1) in the copolymer and (2) in chitosan.

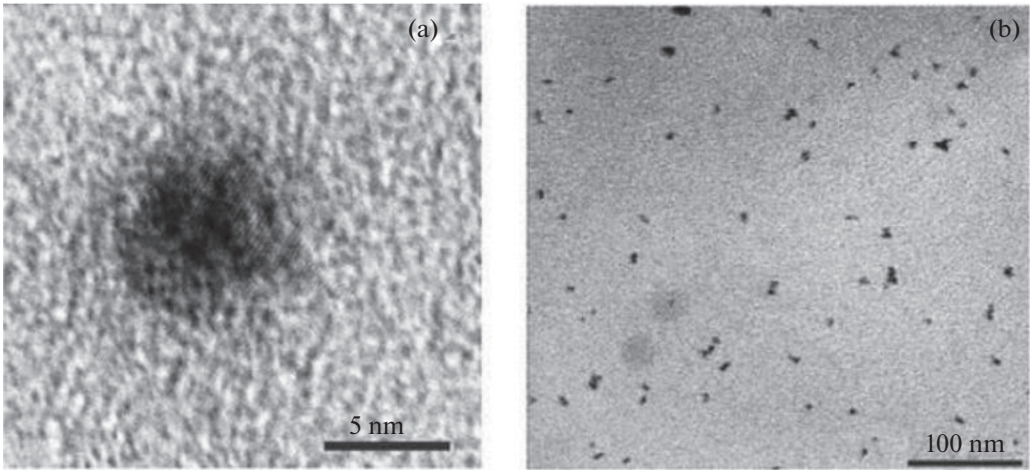

Fig. 9. The SEM microphotographs of the composite with platinum NPs.

The average sizes of platinum NPs in chitosan and copolymer solutions were determined by XPA. XPA diffractograms of the samples show the characteristic peaks of platinum (Fig. 8). The platinum peak width is 2.7° for chitosan and 2.2° for the copolymer. The absorption maxima of platinum in both copolymers were observed at 39.72°. Estimation of the size of coherent scattering regions by the width of the peaks made it possible to calculate the platinum NP sizes in the composition using the Scherrer equation:

$$D = \frac{K\lambda}{\mathrm{FWHM} \times \cos\theta},$$

where D is the crystallite size (Å), K is the so-called "Scherrer constant" (in the present study, $k = 0.94$), λ is the radiation wavelength (0.15418 nm for CuKα), and θ is the diffraction angle of the peak apex. The major "contribution" to the formula is the value of FWHM (Full Width at Half Maximum) of the peaks.

The average sizes of Pt NPs were 4 nm in the copolymer and 3 nm in the initial chitosan. One can see that the UV spectroscopy data are in agreement with the XPA data, and platinum NPs in the copolymer are larger than those in the initial chitosan.

TEM microphotographs clearly show that most of the platinum NPs form agglomerates consisting of several tens of NPs (Fig. 9b). At the same time, individual platinum NPs are characterized by a crystalline structure and an average diameter of about 1.6–5.0 nm NP (Fig. 9a).

Platinum NPs are also detected in thin films of the composites by SEM and recorded on the images as light points (Fig. 10). They have been shown to form

Table 1. The values of inhibitory concentrations (mol/L) of platinum preparations for the cells under study

Cell type	C_{inh} (cisplatin), mol/L	C_{inh} (composite), mol/L
HeLa Kyoto	5×10^{-5}	10^{-4}
A431	10^{-5}	5×10^{-5}
hTERT BJ-5TA	6×10^{-6}	10^{-4}

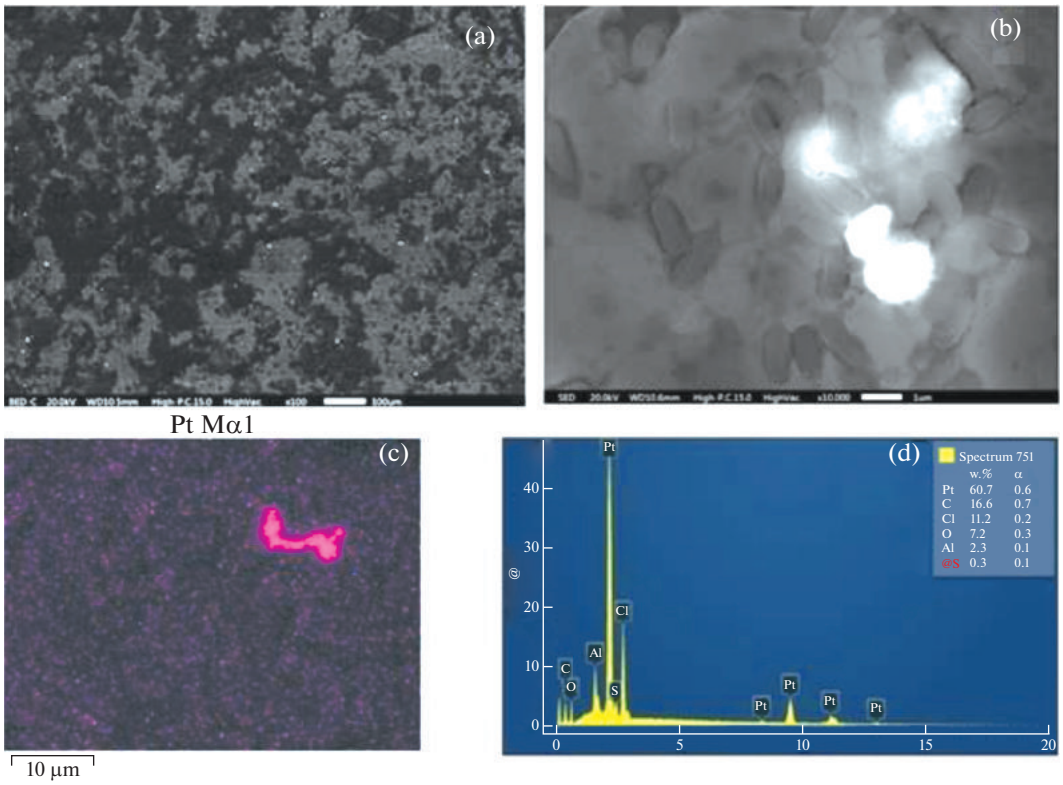

Fig. 10. The SEM images of the composite surface. Light points (a, b, c) are platinum NPs; the diagram (d) demonstrates distribution of elements at the point of the image (c) related to NP agglomerates.

large agglomerates consisting of numerous small NPs; however, their distribution over the surface is uniform. The formation of agglomerates is determined by thin film preparation and drying.

The effect of the composite with platinum NPs stabilized by chitosan–graft–PVP on the viability of HeLa Kyoto and A431 cancer cells has been studied and compared with that of cisplatin (Figs. 11a–11d). The criterion of efficiency was the inhibitory concentration (C_{inh}) at which half of the cells died. In the trials with cancer cells, the lower the C_{inh}, the more effective the substance at fighting cancer cells. The results are presented in Table 1. In the trials with the HeLa Kyoto cell culture, C_{inh} was 5×10^{-5} mol/L for cisplatin and 10^{-4} mol/L for the composite. For A431 cancer cells, C_{inh} was 10^{-5} and 5×10^{-5} mol/L for the composite. In both cases, the concentration of the composite required to inhibit the growth of cancer cells is higher than that of cisplatin. It means that the efficiency of the composite is five and two times less compared to cisplatin for HeLa Kyoto and A431 cell cultures, respectively. However, due to the biocompatible polymer matrix and the lower toxicity of platinum, it was supposed that the composite would be more biocompatible than cisplatin.

The viability of hTERT BJ-5TA fibroblasts was assessed with respect to their adhesion and growth on the surface of composite and cisplatin films (Figs. 11e–11f). The concentration inhibiting fibroblast growth was 10^{-4} mol/L for the composite and 6×10^{-6} mol/L for cisplatin. This probably indicates that Pt NPs stabilized by the copolymer are less toxic than the reference substance, which makes it promising to develop the preparation of platinum NPs in a water-soluble chitosan–graft–PVP polymer matrix with an elevated concentration of the active agent.

* * *

The graft polymerization of VP onto chitosan in an aqueous acidic solution and DMSO has been studied. The optimal conditions for the production of water-soluble grafted chitosan–VP copolymer at a VP content of 80% have been tested. Platinum NPs with an average size of 4 nm have been synthesized in the chitosan–graft–PVP solution at pH 7.0. The antitumor properties of Pt NPs in the chitosan–graft–PVP solution had an efficiency 2–5 times lower compared to cisplatin when tested in vitro in HeLa Kyoto and A431 cancer cell cultures at equal platinum concentrations. It has been demonstrated in the cell culture of hTERT BJ-5TA fibroblasts that a composite with platinum NPs stabilized by chitosan–graft–PVP had an inhibitory effect 17 times lower on the growth of hTERT BJ-5TA fibroblasts compared to cisplatin. It would be

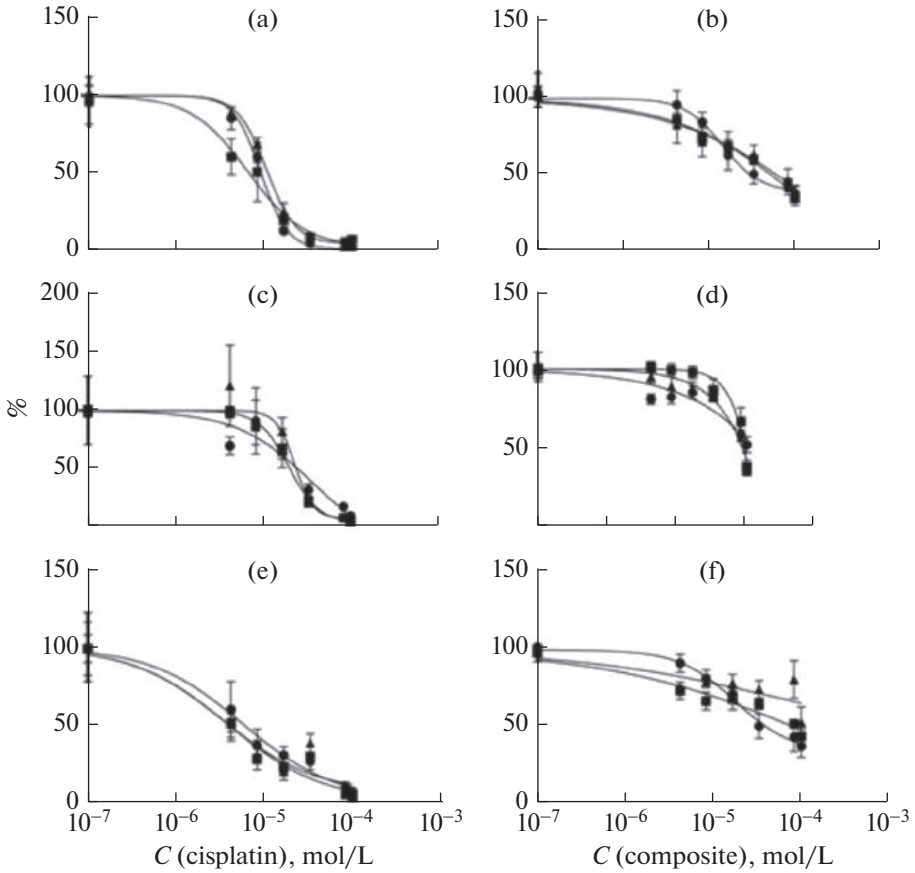

Fig. 11. The viability (%) of HeLa Kyoto cancer cells (a, b), A431 cancer cells (c, d), and hTERT BJ-5TA fibroblast cells (e, f) under the influence of cisplatin (a, c, e) and the Pt NP/copolymer composite (b, d, f).

promising to investigate the composite on the basis of platinum NPs stabilized by chitosan–graft–PVP at higher concentrations of the active agent compared to cisplatin.

FUNDING

This study was supported by the Russian Science Foundation, project no. 23-13-00342, https://rscf.ru/project/23-13-00342/.

ETHICS APPROVAL AND CONSENT TO PARTICIPATE

This work does not contain any studies involving human or animal subjects.

CONFLICT OF INTEREST

The authors of this work declare that they have no conflicts of interest.

REFERENCES

1. Yamada, M., Foote, M., and Prow, T.W., *WIREs Nanomed. Nanobiotechnol.*, 2015, vol. 7, pp. 428–445. https://doi.org/10.1002/wnan.1322
2. Rai, M., Ingle, A.P., Birla, S., Yadav, A., and Santos, C.A.D., *Crit. Rev. Microbiol.*, 2016, vol. 42, pp. 696–719. https://doi.org/10.3109/1040841X.2015.1018131
3. Arvizo, R.R., Bhattacharyya, S., Kudgus, R.A., Giri, K., Bhattacharya, R., and Mukherjee, P., *Chem. Soc. Rev.*, 2012, vol. 41, pp. 2943–2970. https://doi.org/10.1039/c2cs15355f
4. Huang, H., Yuan, Q., and Yang, X., *Colloids Surf.*, vol. 39, pp. 31–37. https://doi.org/10.1016/j.colsurfb.2004.08.014
5. Du, Y.K., Yang, P., Mou, Z.G., Hua, N.P., and Jiang, L., *J. Appl. Polym. Sci.*, 2006, vol. 99, pp. 23–26. https://doi.org/10.1002/app.21886
6. Rai, M., Ingle, A.P., Gupta, I., and Brandelli, A., *Int. J. Pharm.*, 2015, vol. 496, pp. 159–172. https://doi.org/10.1016/j.ijpharm.2015.10.059
7. Yerpude, S.T., et al., *Environ. Res.*, 2023, vol. 231, no. 2, p. 116148. https://doi.org/10.1016/j.envres.2023.116148

8. Khan, M.A.R., Al Mamun, M.S., and Ara, M.H., *Microchem. J.*, 2021, vol. 171, p. 106840. https://doi.org/10.1016/j.microc.2021.106840
9. de la Rosa, S.Y., et al., *Int. J. Mol. Sci.*, 2022, vol. 23, no. 16, p. 9404. https://doi.org/10.3390/ijms23169404
10. Malode, U., et al., *Bull. Natl. Res. Centre*, 2023, vol. 47, no. 1, p. 130. https://doi.org/10.1186/s42269-023-01104-y
11. Kumar, A., Das, N., and Rayavarapu, R.G., *J. Nanotheranostics*, 2023, vol. 4, no. 3, pp. 384–407. https://doi.org/10.3390/jnt4030017
12. Jan, H., et al., *J. Saudi Chem. Soc.*, 2021, vol. 25, no. 8, p. 101297. https://doi.org/10.1016/j.jscs.2021.101297
13. Jeyaraj, M., Gurunathan, S., Qasim, M., Kang, M., and Kim, J., *Nanomaterials*, 2019, vol. 9, no. 12, p. 1719. https://doi.org/10.3390/nano9121719
14. Wang, W., Liang, G., and Zhang, W., *Chem. Mater.*, 2018, vol. 30, no. 10, pp. 3486–3498. https://doi.org/10.1038/s41467-019-09566-3
15. Kutwin, M., *Arch. Med. Sci.*, 2017, vol. 201, no. 13, pp. 1322–1334. https://doi.org/10.5114/aoms.2016.58925
16. Arantseva, D.A., and Vodovozova, E.L., *Russ. J. Bioorg. Chem.*, 2018, vol. 44, no. 6, pp. 619–630. https://doi.org/10.1134/S1068162018060031
17. Moiseenko, V.M., *Prakt. Onkol.*, 2006, vol. 7, no. 3, pp. 170–178.
18. Vartanyan, A.A. and Ogorodnikova, M.V., *Ross. Bioter. Zh.*, 2004, vol. 1, no. 3, pp. 14–18.
19. Akhtyamov, A.E., *Mezhdunar. Studench. Nauchn. Vestn.*, 2018, no. 4, part Z, pp. 4Z6–4Z9.
20. Johnstone, T.C., Suntharalingam, K., and Lippard, S.J., *Prodrugs. Chem. Rev.*, 2016, vol. 116, no. 5, pp. 3436–3486. https://doi.org/10.1021/acs.chemrev.5b00597
21. Panikkanvalappil, S.R., Mahmoud, M.A., Mackey, M.A., and El-Sayed, M.A., *ACS Nano*, vol. 7, no. 9, pp. 7524–7533. https://doi.org/10.1021/nn403722x
22. Zhang, C., Xu, C., Gao, X., and Yao, Q., *Theranostics*, 2022, vol. 12, no. 25, pp. 2115–2132. https://doi.org/10.7150/thno.69424
23. Wennemers, H., Shoshan, M.S., and Vonderach, T., *Angew. Chem., Int. Ed.*, 2018, vol. 58, no. 15, pp. 4901–4905. https://doi.org/10.1002/anie.201813149
24. Varlamov, V.P., Il'ina, A.V., Shagdarova, B.Ts., Lun'kov, A.P., and Mysyakina, I.S., *Usp. Biol. Khim.*, 2020, vol. 60, pp. 317–368.
25. Svirshchevskaya, E.V., Grinevich, R.S., Reshetov, P.D., Zubov, V.P., Zubareva, A.A., Il'ina, A.V., and Varlamov, V.P., *Bionanotekhnol. Nanobiomaterialoved.*, 2012, vol. 1, no. 19, pp. 13–19.
26. Sartaj, A., Qamar, Z, Qizilbash, F.F., Annu, K., Md, S., Alhakamy, N., Baboota, S., and Ali, J., *Polymers* (Basel), 2021, vol. 13, no. 24, p. 4400. https://doi.org/10.3390/polym13244400
27. Panfilova, E.V., Burov, A.M., and Khlebtsov, B.N., *Colloid J.*, 2020, vol. 82, no. 1, pp. 27–35. https://doi.org/10.1134/S1061933X20010093
28. Nie, Z., Petukhova, A., and Kumacheva, E., *Nat. Nanotechnol.*, 2010, vol. 5, no. 1, pp. 15–25. https://doi.org/10.138/ nnano.2009.453
29. Kulikov, S.N. and Khairullin, R.Z., *Vestn. Kazan. Tekhnol. Univ.*, 2015, vol. 18, no. 18, pp. 265–267.
30. Litmanovich, O.E., *Vysokomol. Soed., Ser. C*, 2008, vol. 50, no. 7, pp. 1370–1396.
31. Pourjavadi, A., Mahdavinia, G.R., Zohuriaan-Mehr, M.J., and Omidian, H., *J. Appl. Polym. Sci.*, 2003, vol. 88, no. 8, pp. 2048–2054.
32. Solomko, N.Yu., Dron, I.A., Budishevskaya, O.G., and Voronov, S.A., *Proc. Chem.*, 2009, vol. 1, no. 2, pp. 1567–1575.
33. Hsu, S.-C., Don, T.-M., and Chiu, W.-Y., *J. Appl. Polym. Sci.*, 2002, vol. 86, no. 12, pp. 3047–3056.
34. Arzhakov, M.C., *Termomekhanika polimerov* (Thermomechanics of Polymers), Montreal: Accent Graphics Communications, 2019.

Translated by E.V. Makeeva